

# Modeling Framework for Identification and Analysis of Key Metrics for Trajectory Energy Management of Electric Aircraft

Seumas M. Beedie<sup>\*</sup>, Caleb M. Harris<sup>†</sup>, Johannes Verberne<sup>‡</sup>, Cedric Y. Justin<sup>§</sup> and Dimitri N. Mavris<sup>¶</sup>  
*Aerospace Systems Design Laboratory, School of Aerospace Engineering, Georgia Institute of Technology, Atlanta, GA, 30332, USA*

To prepare for the upcoming entry into service of electric and hybrid-electric aircraft, regulators may have to update or develop new regulations and standards to ensure safe operations of these new vehicles. To ensure public acceptance, these vehicles need to demonstrate an equivalent level of safety consistent with existing regulations. However, the ability to fly in different modes (forward flight, vertical flight) and the different powertrain elements may require significant changes to regulations to ensure that an insightful representation of the usable energy is provided to flight crews. This requires an understanding of the major operational differences between conventional and electric aircraft, and how these differences impact the trajectories a vehicle can fly. For instance, there is no simple analog to fuel gauges for measuring the extractable energy available on board electric aircraft, as energy related metrics can vary with a range of variables, such as component temperatures, battery health, and environmental conditions. It is thus more complex for flight crews to gauge in real-time how much usable energy is available and to figure out which trajectories are feasible with respect to both energy and power. To assess the feasibility of trajectories and quantify the adequacy of novel energy tracking metrics and methodologies, a trajectory energy management simulation environment is implemented allowing the simulation of various energy metrics across a range of vehicles and missions. This allows decision makers and regulators to assess the importance of these metrics for safe operation across a wide variety of missions. The impact of ambient air temperature, battery state of health, and initial battery, motor, and inverter temperatures are assessed for a typical flight mission. It is concluded that state of health, ambient temperature, and initial battery temperature all had significant impacts on the final state of charge and amount of extractable energy. Additionally, at high ambient temperatures and in aggressive climbs, motor temperature limits and inverter temperature limits can sometimes be reached, further complicating the assessment of what can be done with the amount of energy stored on board. Proper management of these constraints is therefore crucial for optimizing trajectories with respect to energy metrics. Future work is proposed regarding further expansion of the framework simulating aircraft with vertical takeoff and landing capability, and flight-dynamics algorithms that will enable simulation of optimal energy mission profiles.

---

<sup>\*</sup>Graduate Research Associate, School of Aerospace Engineering

<sup>†</sup>Graduate Research Associate, School of Aerospace Engineering

<sup>‡</sup>Graduate Research Associate, School of Aerospace Engineering

<sup>§</sup>Research Engineer II, School of Aerospace Engineering, AIAA Member

<sup>¶</sup>S.P. Langley Distinguished Regents Professor and Director of ASDL, AIAA Fellow

## I. Nomenclature

6DoF	=	6 Degrees of Freedom
ALT	=	Altitude
EASA	=	European Union Aviation Safety Agency
eVTOL	=	Electrical Vertical Take-Off and Landing
FAA	=	Federal Aviation Administration
FCS	=	Flight Control System
GA	=	General Aviation
IFR	=	Instrument Flight Rules
IAS	=	Indicated Airspeed
I	=	Current
ISA	=	International Standard Atmosphere
KCAS	=	Knots-Calibrated Airspeed
KIAS	=	Knots-Indicated Airspeed
KPOC	=	Brackett Field Airport
KTOA	=	Zamperini Field
KVNY	=	Van Nuys Airport
KWJF	=	General Wm. J. Fox Airfield
MTOW	=	Maximum Take-Off Weight
OAT	=	Outside Air Temperature
RRT	=	Rapidly Exploring Random Tree
RSM	=	Response Surface Methodology
SOC	=	State of Charge
SOH	=	State of Health
SRTM	=	Shuttle Radar Topography Mission
S/VTOL	=	Short and/or Vertical Take-Off and Landing
TC	=	Type Certificate
TEM	=	Trajectory Energy Management
UAM	=	Urban Air Mobility
V	=	Battery Voltage
VFR	=	Visual Flight Rules
VTOL	=	Vertical Take-Off and Landing

## II. Introduction

As environmental considerations become more and more prevalent worldwide, fully-electric aircraft are becoming an increasingly attractive solution to ensure sustainable operations and to meet increasingly stringent emission reduction targets. New electric offerings have started to appear on the market with the emergence of several models over the past several years, particularly in the niche of small, general aviation (GA) aircraft. The short range requirements, limited power requirements, and emphasis on low operating costs make the GA market ideal for electric aircraft. Updated certification standards are however not yet established in the US for these vehicles, yet to ensure public acceptance, it is critical for these vehicles to demonstrate an equivalent level of safety consistent with existing regulations. To do so requires an understanding of the key operational differences between conventional and electric aircraft, chiefly stemming from the unique requirements of an electric powertrain.

One operational difference is the management of energy and the monitoring of the powertrain performance to achieve a desired mission profile, a concept hereafter referred to as Trajectory Energy Management (TEM). The principle of energy management is well established for conventional aircraft, and the safety benefits have been demonstrated; Puranik et al provide a comprehensive review of the metrics used to quantify energy management for general aviation aircraft [1]. In comparison, the energy management characteristics of electric aircraft are less well understood. To establish an equivalent energy management capability for electric powertrains, different metrics quantifying powertrain performance, power consumption, and energy available must be determined in the context of the types of real-world missions these vehicles will undertake. The sensitivity of these parameters to both environmental and mission parameters is critical to understanding the major operational differences as compared to conventional aircraft.

Modeling an electric powertrain offers a number of challenges. Firstly, the performance of lithium-ion batteries that serve as energy storage can be highly non-linear and heavily dependent on the health of the battery. Secondly, the thermal management required for high-power electrical systems result in changes to the overall system efficiency, which combined with active cooling systems typically on board, result in complex behaviors that cannot always be easily predicted. Finally, the limited specific energy density of current batteries means that most vehicles have limited range capability. In turn, this means that accurate energy and range estimations are vitally important.

These challenges necessitate the development of a modeling framework capable of analyzing relevant powertrain metrics for a fully-electric vehicle across a range of relevant mission profiles. This base level capability will provide a starting point for the implementation of more complex trajectory energy management system, allowing the optimization of trajectories with respect to key energy and power metrics identified in this paper.

In the wider context of developing a full TEM modelling & simulation capability for electric aircraft, this paper focuses on the development of an initial capability intended as a subset of the eventual full framework. This initial capability allows a user to simulate a pre-defined trajectory and then simulates key powertrain metrics along it. In this paper, we detail the development of separate flight dynamics and powertrain models to provide this capability and analyze the performance across a range of missions. In section III, relevant background literature is presented on a range of energy management approaches for different propulsion architectures. Additionally, modeling approaches for electric powertrains are reviewed, with particular reference to NASA's X-57 Maxwell electric demonstrator. In section IV we detail the modeling approach, comprised of the flight dynamics and powertrain modules. In section V we derive and outline the mission profiles that form the basis of the subsequent analysis. In section VI conclusions are drawn and future work to the framework developed and presented is proposed.

To simplify development of the proposed modeling capability, the scope is limited to fully-electric architectures and this research highlights the development of the initial capability with the modeling of a contemporary, commercially available aircraft; the Pipistrel Velis Electro \* across a limited set of mission profiles. Future work will focus on the expansion of the framework to different configurations and mission profiles, including configurations capable of Vertical Takeoff and Landings.

### III. Background

Following increasingly aggressive emission reduction targets, there has been a growing interest in fully or partially electrified propulsion systems. The literature reflects this trend, with a commensurate increase in research papers focusing on modeling and simulation of these new architectures. The focus of the existing literature is overwhelmingly pitched towards hybrid architectures; a review by Brelje et al concludes that from 2015-2019, the volume of papers regarding electric and hybrid electric design and analysis increased by 20% [2]. The emphasis on hybrid architectures is likely due to the limited energy density of currently available lithium-ion batteries. This results in limited range and performance of fully electric architectures compared to their hybrid counterparts, limiting the commercial applications for such vehicles [3, 4]. Still, with every year passing by, the usefulness of fully electric powertrains improves owing to the strides made in energy storage technology by the automotive industry. This research therefore focuses on the modeling and simulation of fully-electric architectures.

Although the behavior underlying electric propulsion elements and their respective models is expected to be comparable between architectures, the hybrid architecture includes additional degrees of freedom inherent to energy management of the aircraft [5]. This stems from the independent usage of combustion and propulsion elements by either the flight control system or pilot to maximize propulsive efficiency over the course of a mission [5]. Such complexities are not present in a purely electric architecture. This greatly simplifies energy analysis, while the energy management metrics used for the electric portion of a hybrid powertrain provide a useful starting point in the analysis of fully-electric vehicles.

A range of fully-electric vehicles are now commercially available, with a wide array of configurations currently in development [4]. However, there exists limited literature on energy modeling and management for fully-electric aircraft, particularly when subject to the unique constraints of an electric powertrain. One of the major bodies of work on this subject was done by NASA using the X-57 Maxwell flight demonstrator aircraft - a conventional Tecnam P2006T airframe modified with an electric powertrain. The studies conducted offer a range of insights; an investigation into the impact of thermal constraints on trajectories was explored by Falck et using the X-57 Mod II (2 60 kW Joby Aviation electric motors) [6]. A model of the electrical subsystems was developed, and using a simple 2D aircraft dynamics

---

\*<https://www.pipistrel-aircraft.com/aircraft/electric-flight/velis-electro-easa-tc/>

model, simulated trajectories were flown subject to thermal constraints. These were shown to be mostly constraining during the climb phase, but considerably less restrictive than the final State of Charge (SOC) requirement.

Building on this work, the initial trajectory generation capability was expanded into a multi-phase mission planning tool, capable of simulating all aircraft trajectory phases: taxi, motor run-up, takeoff, climb, cruise, and descent [7]. Performance parameters are captured at each point of the trajectory, including battery state of charge, component temperatures, and propulsion thrust; these parameters can then be used to influence the trajectory of the aircraft. This was assessed by repeated simulations of a single A-to-B mission profile for a range, as well as preliminary trajectory optimizations attempting to maximize the final State of Charge subject to constraints on power, angle of attack, and acceleration. A potential issue noted is the linearly interpolated mission profiles resulting in a constantly varying throttle, which is unlikely to be how to aircraft is realistically flown. This work demonstrates the impact of considering power and thermal metrics in two potential ways - whether or not these considerations disqualify a potential trajectory, or whether they are used to optimize an existing one. The scope of the research will focus on the former: developing trajectories to assess based on simulated energy and power metrics. The trajectory optimization is intended to be completed in the next phase of this research.

The body of modeling and simulation research conducted on the X-57 provides key insights into aspects of trajectory management for an electric powertrain. Although the X-57 has proved a crucial test-bed for a host of electric aircraft technologies, it is not necessarily representative of the electric aircraft available on the commercial market. In contrast, this research models a commercially available 2-seat GA aircraft that offers a more contemporary baseline. A 6 Degrees of Freedom (6DoF) aircraft model (validated with real flight test data) is used to expand the scope of the previous research by enabling 3D trajectories to be flown, and simulate a range of additional energy metrics.

The battery model is borrowed from an earlier NASA work by Chin et al on the modeling of battery performance; a complex task due to the multivariate non-linearity of lithium-ion batteries. A physics-based equivalent circuit model is used to characterize the electrical performance of the battery; a rather common approach in the literature [4]. These types of models are highly dependent on the laboratory experiments used to determine equivalent component values, and it is difficult to verify that these experiments will yield results applicable to the stochastic environment encountered by the aircraft during real-world missions [8]. For a TEM environment designed to analyze power and energy over a given mission profile, an approach that can account for this uncertainty is needed. For this research, access to flight test data allows the creation of a component-level surrogate models that constitute an overall powertrain model - ensuring the models of powertrain components are representative of real-world operating conditions.

This is addressed in the existing literature primarily through a range of state estimators, allowing the physics-based predictions to be corrected with uncertainty estimates drawn from covariances matrices characterizing the joint variability between combinations of state and model parameters [9]. Two particularly prevalent variations of this approach that emerge throughout the literature are the use of the Extended and Unscented Kalman filters, which broadly speaking apply the principle of Kalman filtering to nonlinear systems - better suited to the nonlinear behavior of the electric powertrain [10]. These kinds of probabilistic approaches are primarily focused on developing a modeling capability for on-line estimation, intended to provide a real-time management information to the pilot; this objective places requirements on the models, placing a high premium on model fidelity not required to assess metrics like State of Charge that are integrated over an entire mission profile. Therefore, a simplified approach with a premium on computational speed is better suited for the rapid analysis of many mission profiles.

In summary, there exists a gap in the literature for the development of modeling & simulation capabilities specifically for the kinds of fully-electric aircraft now entering the market. This capability also provides the basis for the development of a full TEM framework to fill another gap in the literature; the unique problem of energy management specific to fully-electric aircraft.

#### **IV. Modeling Framework**

To achieve the aforementioned modeling & simulation capability, the trajectory energy modeling component of the simulation environment is split into two main components: trajectory generation, and energy analysis. The trajectory generation component inputs the desired mission profile, determined from the mission objectives and a vehicle representation. The flight dynamics component of the environment will then use this information to generate shaft power requirements for a given timestep. The shaft power required for a set duration (a user defined input) is then fed into the second key component, the energy analysis, which utilizes a hybrid approach of physics-based and response surface methodology (RSM) surrogate powertrain component models to convert this power requirement into a rate of change of battery SOC (a derived energy-related metric discussed in the powertrain modeling section), which can

be integrated over the timestep to yield a change in SOC to be subtracted from the initial value. This architecture is depicted visually below in Figure 1.

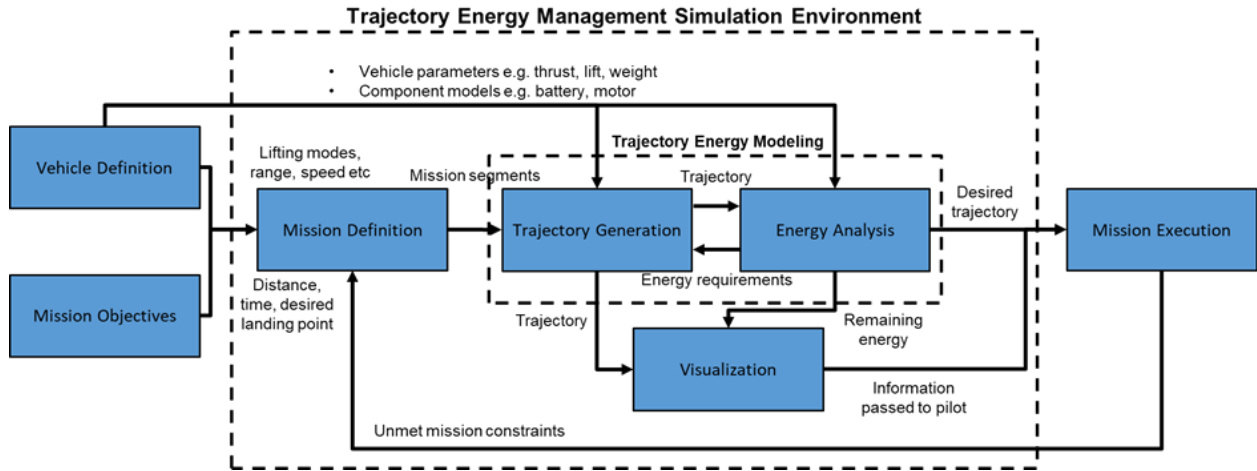


Fig. 1 Overall Trajectory Energy Management (TEM) simulation environment architecture

### A. Notional Vehicle

To understand the requirements of real-world electric aircraft, a representative aircraft is used throughout this research. The Pipistrel Velis Electro is a Slovenian two-seater GA electric aircraft and also the world's first electric powered airplane to receive a Type Certificate (TC) from EASA in June 2020 (EASA.A.573 Type Certificate Data Sheet) for day, VFR operations [11]. The design was certified as a variant of the Pipistrel Virus, an airframe developed for a conventional powerplant [12].

The aircraft utilizes an electric motor producing a rated maximum takeoff power of 57.6 kW at 2500 RPM for 90 seconds. It is powered by two 11.0 kWh lithium-ion batteries connected in parallel, supplying direct current to a liquid-cooled inverter, providing the necessary alternating current to the motor. The battery and inverter feature liquid cooling, while the motor relies on passive airflow.

The Velis features a 10.71 m wingspan, giving a total wing area of 9.51 m<sup>2</sup>. An empty weight of 428 kg and a maximum payload of 172 kg which gives a total MTOW of 600 kg. At this weight, the vehicle is capable of a maximum speed at sea level of 98 KCAS, and a cruise speed of 90 KCAS at a power setting of 35 kW. At the best climb speed of 75 KIAS, the aircraft can reach a service ceiling of 12,000 ft (3660 m), and can achieve a maximum endurance of 50 minutes (plus VFR reserve). The aircraft is shown in flight in Figure 2 [13].

### B. Powertrain Modeling

Once a trajectory has been generated from the mission requirements to be shown in the next section, it can then be provided as an input to the powertrain model. The purpose of the model is to fly the defined trajectory, and given a set of initial conditions which determine the health and charge of the battery, simulate energy and power related metrics throughout the course of the mission. To quantify the remaining energy on-board the aircraft, two metrics are utilized: State of Charge (SOC), and available energy.

#### 1. Energy Metrics

Available energy can be objectively measured in kWh, and can be calculated from simulated battery electrical parameters such as current and voltage. In contrast, SOC is a derived metric that cannot be easily measured or calculated from electrical parameters, and requires a brief review - given subsequently. SOC is the established metric for assessing the energy remaining in a battery, giving a dimensionless ratio of the current battery capacity to the maximum charge. Note that this is the maximum charge the battery can hold for its given State of Health (SOH) value, as opposed to the nominal maximum charge when it was new. As the health of the battery changes, this changes the SOC, and thus SOC values cannot be directly compared between two batteries with different SOH values. As a dimensionless quantity,



**Fig. 2 The Pipistrel Velis Electro Aircraft in Flight**

SOC cannot be directly measured, and instead relies on an abstraction of several important parameters that affect the rate of discharge, such as voltage, current draw, and cell temperature. In spite of the drawbacks, SOC remains the metric of choice for assessing available battery energy, and consequently there is a large body of literature concerning estimation methods. A range of traditional SOC estimation methods exist, and are broadly categorized by Hannan et al [14]. Of these methods, model-based estimation, data-driven estimation, or a hybrid method (combining the former two) are the most directly applicable for a simulation tool (where voltage and current cannot be directly measured). Model-based estimation relies on differential equations to model underlying processes; these can be purely electrical (equivalent circuit model), electrochemical, or a combination. They are accurate, but often computationally expensive, and require extensive knowledge of underlying phenomena, which is not always the case – particularly when operating at temperature extremes. Data-driven estimation uses trained algorithms derived extensive datasets. Although less dependent on understanding the underlying phenomena, this requires a large amount of good quality data to instead mathematically approximate the underlying behavior.

## *2. Modeling Methodology*

Using flight test data made available by Pipistrel for this research, selecting a data-driven approach offers a number of benefits over a physics-based approach. Firstly, the superior computational speed offered by the evaluation of low-cost surrogate models is important for the eventual development of a full TEM framework, which will be required to rapidly analyze a large number of trajectories. Secondly, use of real-world training data to generate the models ensures the simulation is reflecting the aircraft in real operating conditions, as opposed to the equivalent circuit models that must be characterized with laboratory data. Response Surface Methodology (RSM) surrogate models were used to train the individual component-level models that comprise the overall powertrain model. This allows a large number of factors and interactions to be considered for each model, while still retaining a low evaluation cost that will be critical for full trajectory energy management. In order to train the model, data from six different flight missions were aggregated into a single data set to ensure points can be sampled from each mission, without an over-reliance on any specific one. Least-squares fits were used for all models, with a 75/25 training-validation split of the aggregate dataset. The model must contain representations of the key modular components that comprise the powertrain. This will allow a final model architecture to be generalized across a range of partially or fully electric architectures, including S/VTOL vehicles, where architectures can be defined by combinations of powertrain elements in series and/or in parallel. As defined earlier, for the Pipistrel Velis Electro, these are two parallel batteries (modeled as one) connected to a motor-inverter pairing providing shaft power to a fixed-pitch propeller. The specific modeling of each of these is detailed subsequently, along with the individual thermal models for each component.

### 3. Propeller Model

The flight dynamics model estimates required thrust which is passed to the powertrain model and where it is converted to a requested torque (up to a maximum of 220 Nm). For a propeller driven aircraft however, this must be converted to a shaft power requirement from the motor. To obtain this, an estimate of motor RPM is required - typically obtained from a propeller model. However, for the initial capability to identify and analyze powertrain metrics, development of a full propeller model was considered out of scope. To obtain an RPM estimate, a response surface surrogate model was trained over the aggregate flight test data, taking IAS, ALT, OAT, and requested torque as inputs. An R-squared value of 0.98 was obtained with a least-squares fit, indicating a good fit.

### 4. Motor/Inverter Model

The motor/inverter pairing is represented with one component-level model, with the inverter also constituting the motor controller. This inputs torque and RPM values from the propeller surrogate, the flight dynamics outputs (IAS, OAT, altitude), and component temperatures, and uses two independent RSM surrogate models to predict current and voltage respectively, as required by the motor/inverter, and as seen by the battery model. Each surrogate has an R-squared value of 0.99 for both the training and validation sets for the aggregated Pipistrel dataset, indicating a strong interpolative confidence within the parameters of the training missions.

### 5. Battery Model

The surrogate model representing the battery maps the current and voltage from the motor/inverter model to desired energy-based metrics: SOC and available energy. To obtain SOC, while accounting for the impact of SOH, an RSM surrogate predicts the % SOC consumed per unit change consumed for a given SOH, which when multiplied with the total charge consumed yields the updated SOC. A second RSM surrogate is used to predict thermal power wasted (functionally equivalent to the electrical resistance of the powertrain multiplied by the square of the current, yielding a power quantity). A running total of energy consumed is obtained by integrating the charge and voltage over the course of the mission, which when combined with the predicted wasted thermal power, yields the total extractable energy (in kWh) for the given power setting. Note that for the Velis Electro, energy is provided by two batteries connected in parallel, each with a nominal energy of 11 kWh. These batteries are independent, and each provide approximately half of the current draw simultaneously, resulting in nearly identical performance for each battery. The greatest discrepancy between battery temperatures observed in the flight test data was 4 degrees Celsius, therefore for this research, only one battery is simulated, with the assumption that the second battery behaves similarly.

### 6. Thermal Modeling

As demonstrated by Falck et al [6], when thermal constraints are considered - particularly in climb - there is a significant impact on the resulting optimal trajectory. Therefore it was considered vital to independently model the temperature of the battery, motor, and inverter, allowing the impact of each to be independently quantified. Once a full TEM capability has been developed, the individual component temperatures will also provide constraints that can be used to generate trajectories. RSM surrogate models were trained over the aggregate dataset, predicting the rate of temperature rise (in degrees Celsius per second) as a function of IAS, OAT, altitude, motor RPM, requested torque, initial temperature, and the average charge consumed over the last 10 seconds. This last input provides a measure of the average power consumption over a small time window; this accounts for situations where the instantaneous current drops quickly, but the thermal energy from immediately previous current draw has not had time to dissipate. The temperature values are updated with every step of the model, and feed into the relevant component models. The powertrain model architecture for the Velis Electro can be seen in Figure 3.

## C. Trajectory Generation

A predictive method is necessary to determine the power and energy draw during the flight. Therefore, a trajectory generation tool is developed to combine terrain data, weather data and vehicle dynamics to produce visualizations of accessible trajectories with predictions of energy remaining. The modular design of the dynamics model through aerodynamic derivative calculations, as well as the tool's definition of the trim and flight modes, allows for the modeling of conventional takeoff and landing vehicles as well as vertical takeoff and landing vehicles in future analysis. Trajectories are generated using a discrete set of trim conditions for a fixed-wing vehicle and are restricted by energy requirements and terrain obstacles.

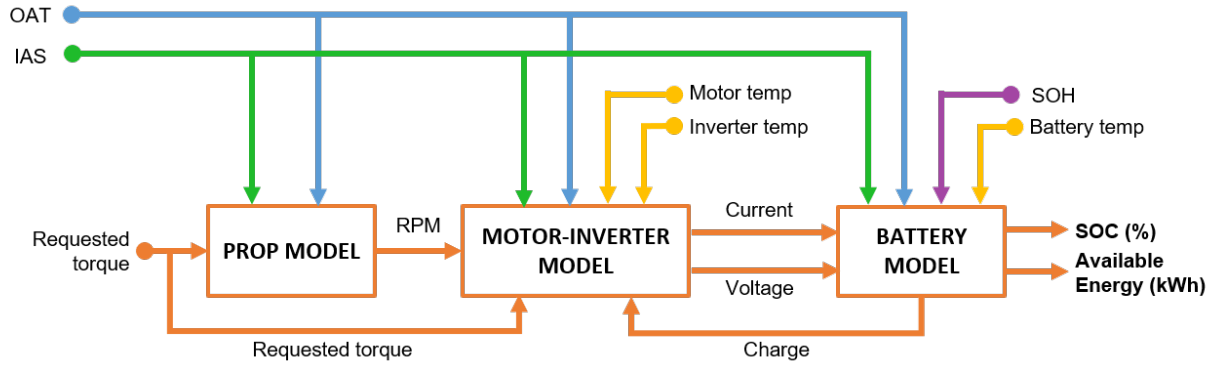


**Fig. 3 Powertrain Model Architecture for the Pipistrel Velis Electro**

### 1. Environment Data

The flight of electric vehicles is often at low-altitude for UAM and other similar missions. Therefore, a critical area of energy use is in avoiding the terrain or other obstacles in the environment. In addition, satellite and map data have become increasingly accessible through both open-source and paid services, allowing for the simulation of flights through these regions with accurate data in the region of interest.

This work uses radar elevation data from the Shuttle Radar Topography Mission (SRTM)<sup>†</sup>. The GMTED2010 SRTM dataset has 7.5 arcsec resolution, resulting in a 264 MB dataset for entire western half of the United States. Figure 4 shows the SRTM data for Los Angeles where lighter colors show higher terrain. This environment data can be used by the trajectory generation tool to produce viable trajectories that can be used to facilitate the powertrain analysis. Terrain collision detection is done in two different ways, depending on the task. Either the terrain data is projected onto a discretized coordinate system where the flight model will operate, or the flight trajectory is projected into the Geographic Coordinate System of the terrain data.

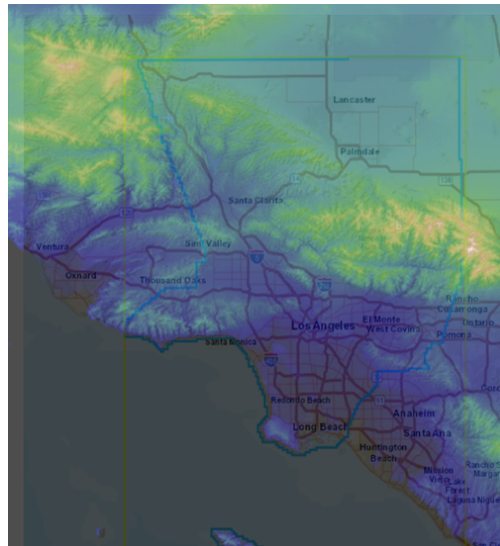


**Fig. 4 Los Angeles SRTM Elevation Data**

### 2. Dynamics Model

A medium-fidelity, fixed-wing aircraft was selected as the dynamics model of interest. A 6 degrees-of-freedom (6DoF), rigid-body dynamics model of a fixed-wing electric vehicle was defined using the equations of motion and

<sup>†</sup><https://lpdaac.usgs.gov/products/srtmgl3v003/>



aerodynamic derivatives from Stengel [15]. The vehicle is defined and its dynamics are forward propagated by the use of its aerodynamic derivatives. A simplified set of control inputs allow for trajectories to be formed, which are feasible or even optimal to a set of energy or acceleration objectives. The physics model itself confirms that the trajectories are held to the dynamics constraints.

The dynamics model is defined in the simulation environment with a 12-state vector,  $\mathbf{x}$ . The state is divided, in order, as the body-axis velocities, the earth-axis positions, the body-axis angular rates, and the earth-axis Euler angles as shown in Equation 1. The Earth-fixed, body, and wind reference frames are all used for dynamics propagation and are seen in Figure 5. As shown in Equation 1, the control vector consists of four inputs; the elevator deflection, aileron deflection, rudder deflection and the normalized throttle input. These control inputs correspond to the conventional control inputs found on general aviation aircraft and allow for the aircraft states to be changed in the 6DoF simulation.

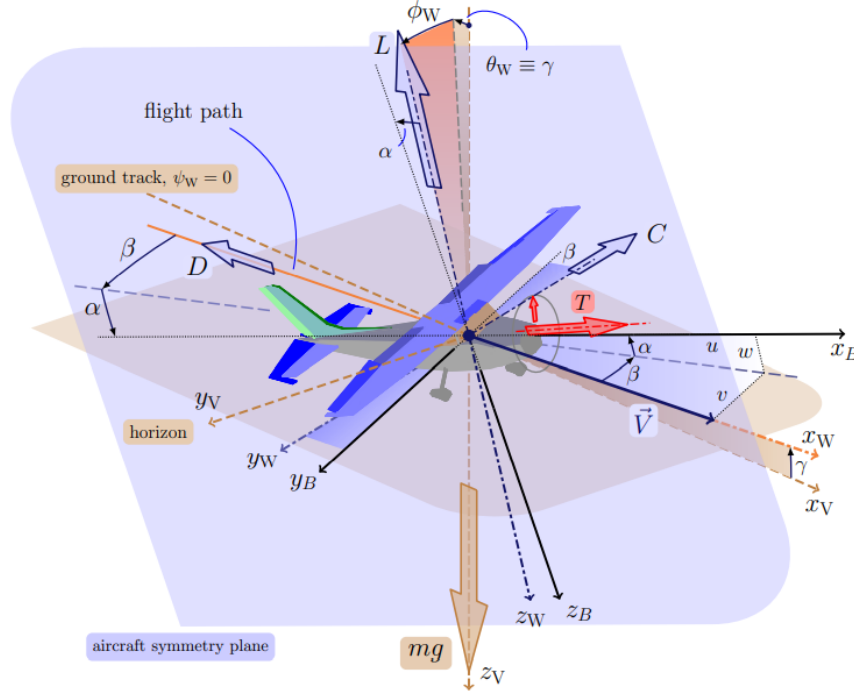


Fig. 5 Aircraft Reference Frames and Definition from [16]

$$\begin{aligned} \mathbf{x} &= [u, v, w, X, Y, Z, p, q, r, \phi, \theta, \psi] \\ \mathbf{u} &= [dE, dA, dR, dT] \end{aligned} \quad (1)$$

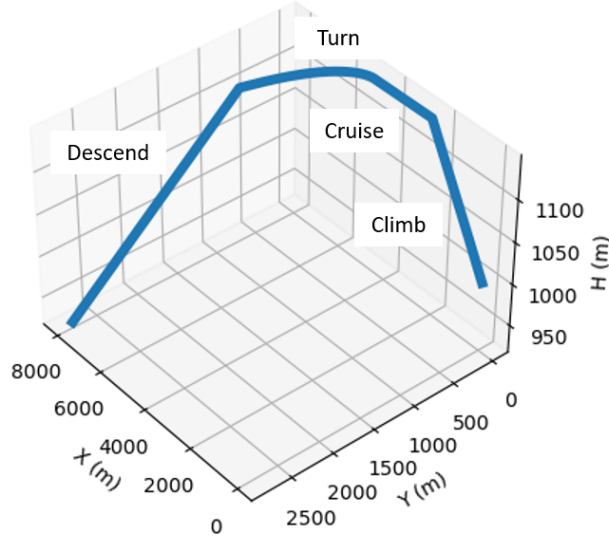
A literature review is performed to retrieve the vehicle parameters used to model the baseline aircraft, while the weight and inertia parameters are approximated using a similar class of general aviation aircraft. A summary of the main parameters needed is given in Table 1.

A series of trim methods for cruise, climb, and turn, modified from [16], are used to maneuver the vehicle and determine power requirements. The trim for cruise, climb, descend and turn are setup as optimization problems, where we seek to minimize acceleration, while achieving the desired flight condition parameters, by searching for the aircraft orientation and input controls that satisfy the vehicle dynamic constraints. The desired flight condition parameters provided by the user to the optimization algorithm consist of the flight path angle and flight velocity. Additionally, the climb and turn segments allow for the specification of the desired rate-of-climb and rate-of-turn. The descend segment uses 0 throttle input to mimic the behavior observed in the series of flight test data used. The optimization algorithm use these desired user-defined inputs to find a stabilizing aircraft orientation and control input. Flight of the fixed-wing aircraft is simulated using the concatenation of these individual cruise, climb, turn and descend trim segments. The

**Table 1 Baseline Vehicle Parameters**

Parameter	Value	Parameter	Value
Wing Area (S)	9.51 m <sup>2</sup>	X-Mass Moment of Inertia ( $I_{xx}$ )	1070 kg · m <sup>2</sup>
Parasitic Drag Coefficient ( $C_{D,0}$ )	0.028	Y-Mass Moment of Inertia ( $I_{yy}$ )	1249 kg · m <sup>2</sup>
Induced Drag Coefficient (K)	0.07	Z-Mass Moment of Inertia ( $I_{zz}$ )	2312 kg · m <sup>2</sup>
Wingspan (b)	10.71 m	XZ-Product of Inertia ( $I_{xz}$ )	-100 kg · m <sup>2</sup>
Max Takeoff Weight (MTOW)	600 kg	Length C.G. to Aero Center H.T. (LHT)	1.73 m
Static Margin	0.25	Length C.G. to Aero Center V.T. (LVT)	1.56 m
Mean Aerodynamic Chord ( $\bar{c}$ )	5.25 m	Equivalent Static Thrust (T)	1300 N

transition between these segments is assumed to be instantaneous such that any transient behavior that results from changing trim conditions is omitted due to the absence of a stabilizing flight controller. An exemplary flight profile can be seen in Figure 6 where a flight is shown for subsequent climb, cruise, turn and descend segments. Figure 7 shows the vehicle inputs to assure successful trimming in each of these segments.

**Fig. 6 3D Flight Profile in Vehicle Simulation**

### 3. Trajectory Formation

In order to facilitate the powertrain analysis of the aircraft model, trajectory formation must be applied to construct realistic use cases that can be analyzed. The individually defined trim segments for cruise, turn, descend and climb allow for the creation of these trajectories. The main focus of the trajectory formation is to generate flight profiles that approximately represent real-world missions. The generated flight trajectories act as an input to the powertrain model, and since the response of the powertrain model is integrated over time, the smaller transients in the flight mission are not of particular interest.

The trajectory generation capability ideally consists of the solution to a two-point boundary optimization problem. The problem can be solved using techniques such as optimization-based methods, grid-based methods, or sampling-based methods. Optimization-based methods such as from optimal control theory can be used to find energy-optimal flight paths for aircraft, as in [17], however they can be complex to define and costly to compute. Grid-based methods use a discretized grid in the search space that may limit the accuracy of the path, but can produce collision-free and optimized paths, such as by using Markov Decision Processes as in [18]. Sampling-based methods are a stochastic technique, which can guarantee completion and sometimes guarantee optimality, while utilizing random graph structures that at

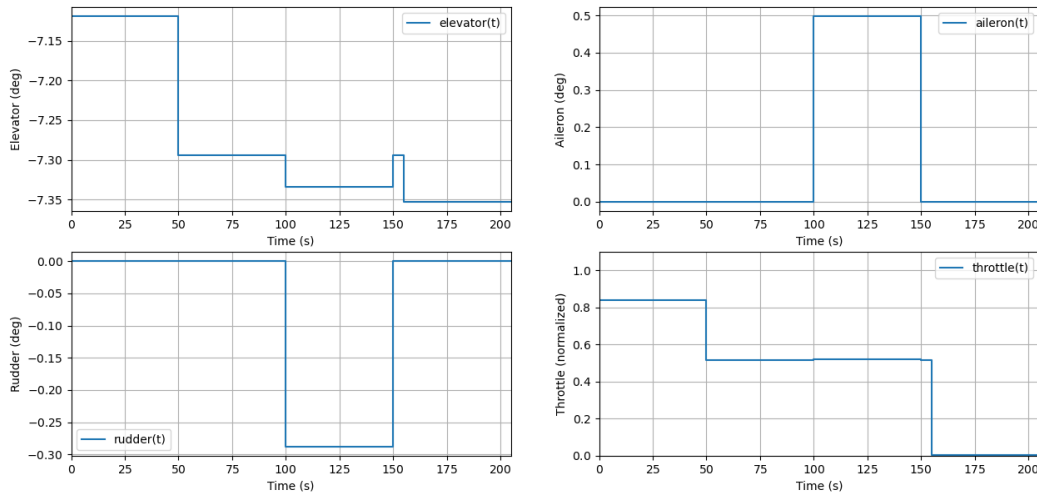


**Fig. 7 Vehicle Inputs in Vehicle Simulation**

times are more efficient than grids, as demonstrated by using probabilistic roadmaps in [19].

Rapidly Exploring Random Tree (RRT), introduced in [20], is a sampling-based method suited to find optimized trajectories between two points. This technique has been used for path planning for aerial vehicles in a wide range of applications ranging from collision avoidance [21], alternative landing [22] and exploration [23].

A first iteration of the original RRT algorithm which seeks to minimize euclidean distance for trajectory optimization is shown in Figure 8 where an exploration tree is shown in black and a found optimum solution path in red. Not shown in Figure 8 is the obstacle field ensuring the RRT exploration follows a minimum climb rate and cruise altitude. By defining the inherent optimizer of the RRT algorithm to minimize energy expenditure, an optimum path can be found between two locations for an electric aircraft mission. An additional application envisioned for the RRT trajectory generation in this research is the exploratory mode in which a real-time map of the surrounding area is constructed and updated to provide information about aircraft range and the reach-ability of surrounding airports and helipads.

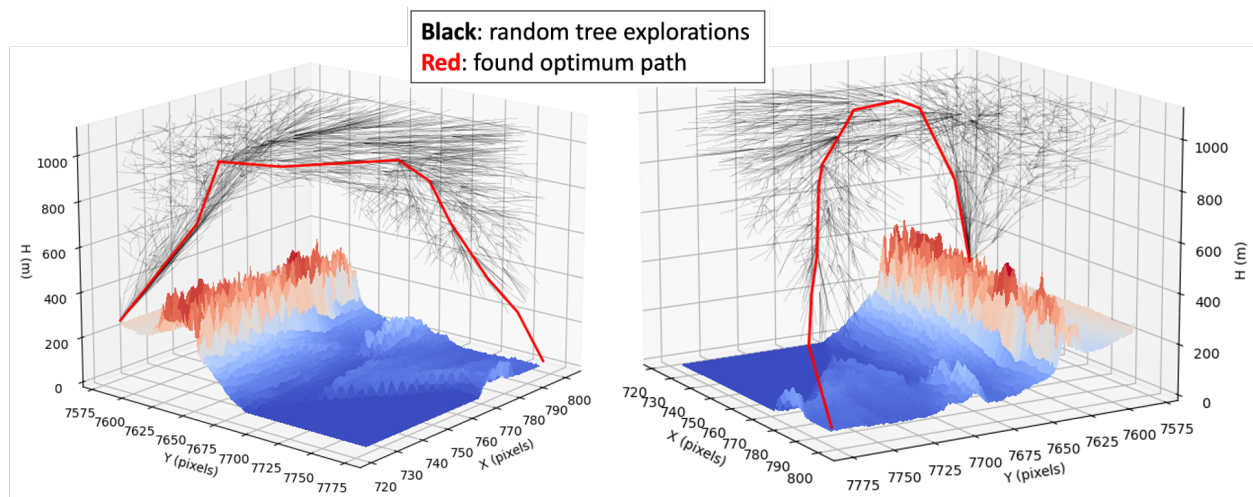


**Fig. 8 Test Case for using RRT Optimized Trajectory Generation**

The addition of a dynamics model and energy-based optimization into RRT complicates the scenario formation and user-defined parameters of interest for this research. Therefore, we first focus on trajectories constructed using a manual

definition of individual trim segments for cruise, climb, descend and turn to clear terrain and navigate to a desired destination using a realistic flight profile similar as shown in Figure 6. The current trajectory formation approach does not result in trajectories that are optimized for energy consumption, but instead focuses on providing realistic trajectories for analyses under a set of changing parameters and metrics.

#### 4. Wind Model

A simple wind model has been created in order to simulate the effect of wind on the vehicle. Since this research is in essence an investigation in range capabilities of electric aircraft and since no stabilizing vehicle controller is applied, the wind effect is modelled as an offset to the ground displacement vector as can be seen in Figure 9. The Wind vector  $\vec{W}$  consists of three wind elements in the North-East-Down reference frame that are subsequently added to the vehicle velocity vector,  $\vec{V}_{velocity}$ , to produce the ground displacement vector,  $\vec{V}_{ground}$ . No wind acceleration elements, neither translational nor rotational, are considered in this application due to absence of a stabilizing flight controller. This definition allows for the capability to vary the wind direction and evaluate its effect on range performance of the electric aircraft of interest.

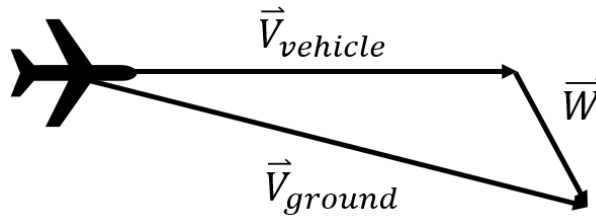
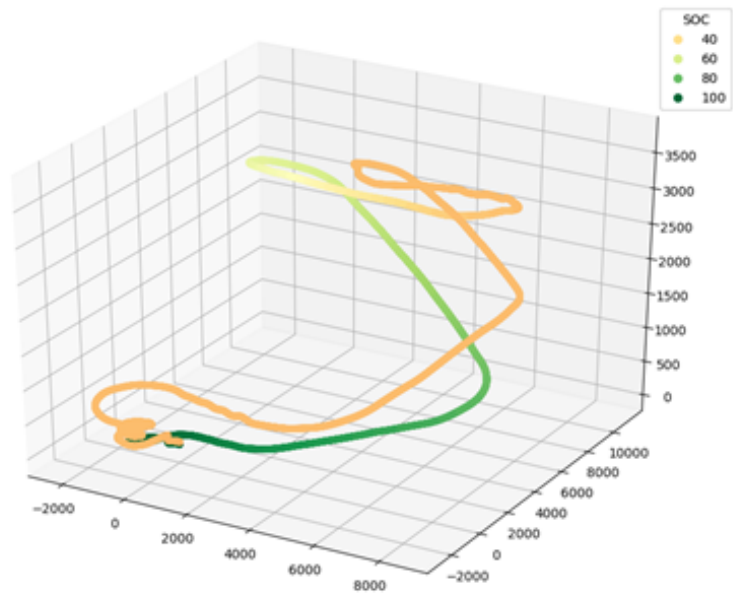


Fig. 9 Wind Field Definition

#### D. Validation

Validation of the integrated environment is required to ensure accuracy and repeatability of the modeling framework when run across a range of missions. To achieve this, of the 7 flight test data logs originally provided by the Pipistrel, one was set aside for validation, while the rest were used to train the powertrain models. The reserved mission is a training mission flown by an experienced pilot, where the aircraft is subject to a long period of maximum continuous power while climbing to the rated service ceiling of 10,000 ft. This provides a validation mission that will test the extremes of the model behavior, particularly at a high power consumption, while still representing a feasible mission that can be flown by the aircraft. The mission was recreated manually using a combination of cruise, climb, turn, and descend segments, and flown at the same conditions as the real flight, with an initial SOC of 98%, and a SOH of 87%, flown at ISA -5 degrees Celsius.

The real and simulated trajectories for this mission are depicted below in Figure 10 and 11 respectively. It can be observed that the simulated trajectory loosely approximates the actual trajectory. Although the manual recreation of the mission results in a sharper trajectory, the overall flight pattern offers an adequate recreation for validation purposes. The simulated powertrain results are plotted in Figure 12, with the actual flight test data plotted in Figure 13. The blue lines indicate data recorded by Pipistrel in flight, and the red dotted lines indicate the simulated analog using the flight test data inputs to the powertrain model. The results of the validation test show that the model approximates the environment, flight, and powertrain conditions, and more importantly closely matches the energy use along the flight. Therefore, the flight dynamics and powertrain models can provide accurate insight to trajectory energy management by running test scenarios, as done in the following section.



**Fig. 10** Actual Trajectory Flown for Validation Mission Flown by Pipistel Velis Electro

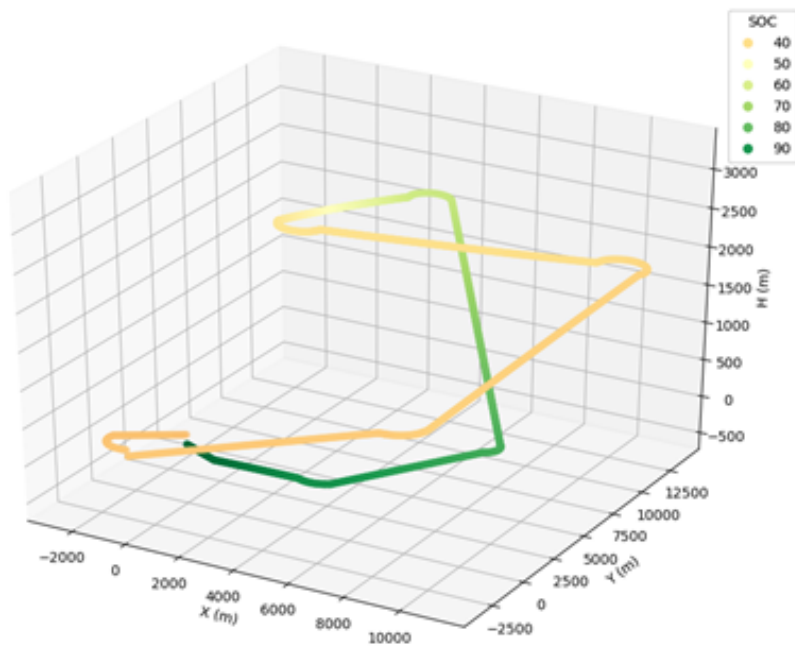


**Fig. 11** Simulated Trajectory Flown for Validation Mission Flown by Pipistel Velis Electro

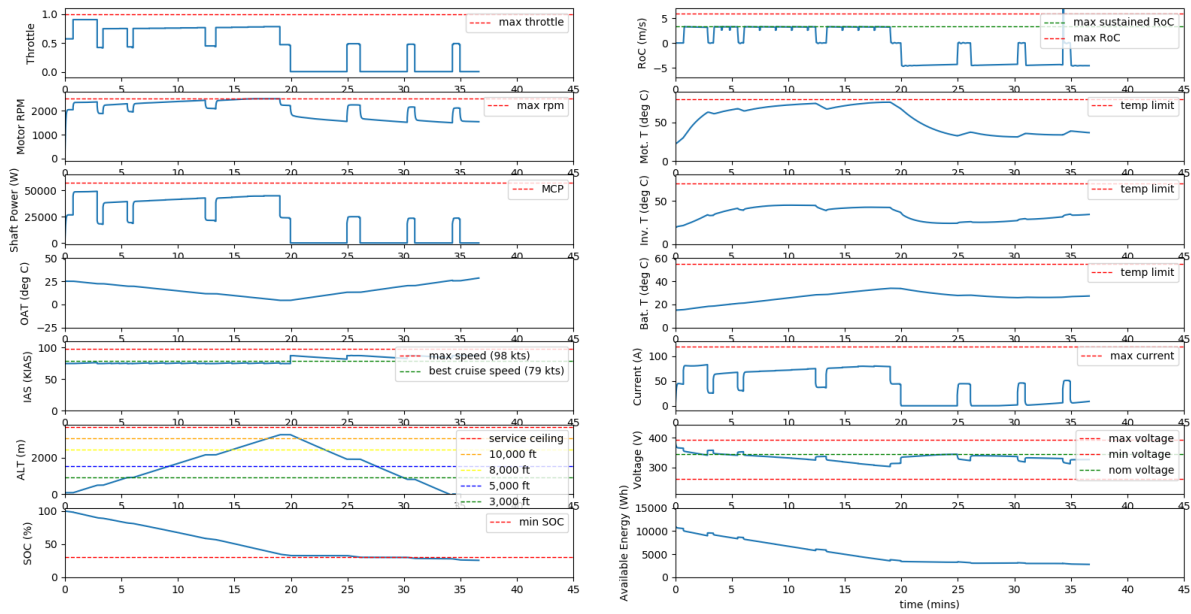


**Fig. 12 Simulated Powertrain Metrics for Validation Mission Flown by Pipistel Velis Electro**

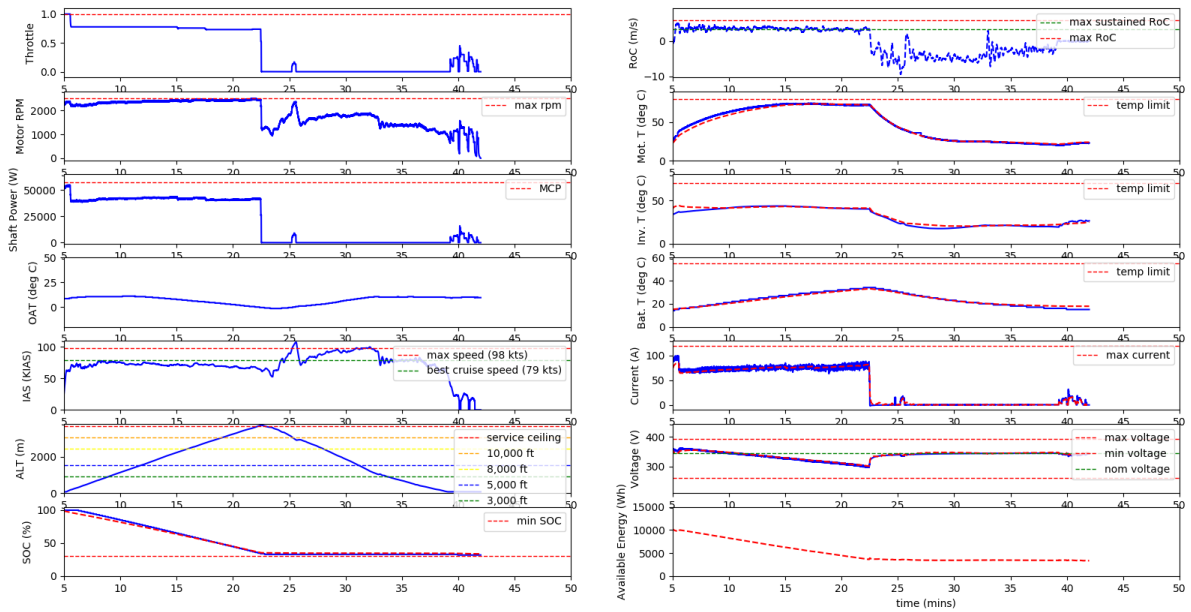


**Fig. 13 Actual Powertrain Metrics for Validation Mission Flown by Pipistel Velis Electro**

## V. Results

The modeling framework developed has the capability to analyze the key metrics for hundreds of trajectories rapidly, providing insight to the effect of various types of missions and environmental conditions during flight. However, the framework can also be used to provide a much more detailed analysis of a specific trajectory defined by the user. This allows a higher level of fidelity, at the cost of computational speed, and can be used to assess the impact of various parameters on the success of a given mission. As the definition of mission success is specific to the type of mission flown, this analysis must be conducted for a singular, feasible trajectory. As these trajectories are intended to represent the kinds of real-world missions flown by small electric aircraft similar to the notional two-seater in this paper, GAMA Publication 16 (Hybrid & Electric Propulsion Performance Measurement)[24] was used to provide a baseline for these missions. Two GAMA profiles were selected, an A to B destination trip (representing a transportation mission), and a local A to A flight (representing a training mission), two of main mission types typically flown by GA aircraft. Los Angeles was selected for demonstration purposes for this research. LA makes for an appropriate case study for multiple reasons. Firstly, Los Angeles has a large population and is notorious for its severe traffic congestion which could be alleviated by UAM operations. This is further supported by the observation that a relatively large group of wealthy people call reside in LA who could be an excellent initial target audience for UAM. Secondly, LA has strict environmental regulations that would support zero-emissions electrified flight. Finally, the Los Angeles area offers a diverse mix of terrain and weather that can showcase the capabilities of the TEM tool.

### A. KVNY to KTOA

This flight is performed between Van Nuys Airport (KVNY) (34.20981, -118.48998) and Zamperini Field (KTOA) (33.80339, -118.33962) to simulate a 20 minutes commuting flight. These trajectories can be seen in Figure 14 where the pentagon shows the location of KVNY and the cross the destination airport KTOA. Units of the figure are in pixels to facilitate image extraction from the terrain file. Additionally, nearby airports 'A' and heliports 'H' are identified. Figure 15 shows the 3D trajectory of the route. Figure 16 shows the simulated powertrain metrics for this canonical mission, and these are the metrics that will be subsequently generated for all flights analyzed in this work. The left column, from top to bottom, shows the throttle setting (as a decimal from 0-1), motor RPM, required motor shaft power (kW), OAT (degrees Celsius), KIAS, altitude (m), and SOC (%). The right column, from top to bottom, depicts vertical rate of climb (m/s), motor temperature, inverter temperature, battery temperature (all in degrees Celsius), battery current, battery voltage, and finally the instantaneous available energy (kWh).

For this canonical mission, a sweep of parameters of interest was conducted to assess the initial importance of these parameters. The initial OAT was varied from -10 to 40 deg C (ISA -25 to +25) - note that the ambient temperature still scales according to the ISA with altitude. The final SOC drops from 72% to 64% at the lowest, a total fluctuation of 8% as can be seen in Figure 17. The yellow points depict runs where the motor temperature limit was exceeded - this occurred at OAT in excess of 36 degrees Celsius.

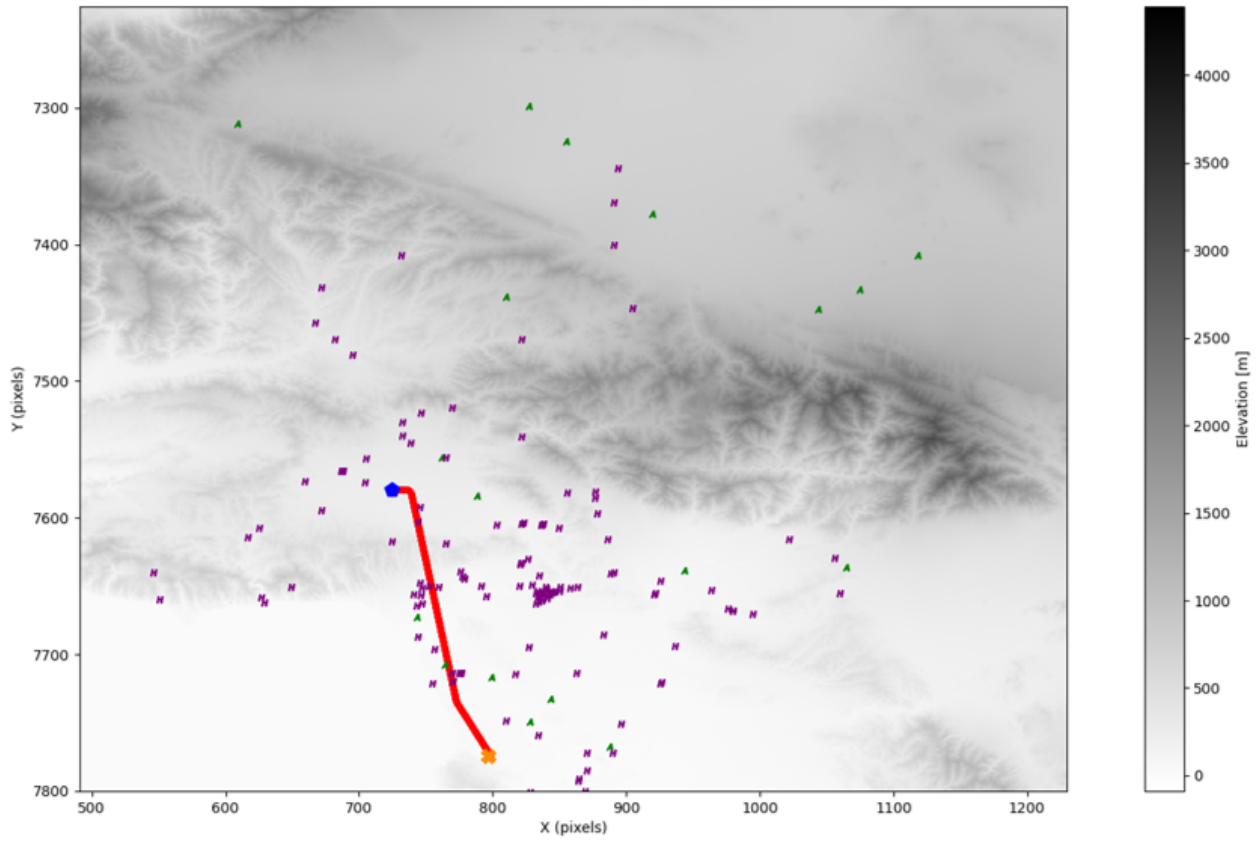
Figure 19, 20, and 21 represents the impact of differing initial component temperatures. It can be observed that the battery temperature constitutes the most significant impact, with both motor and inverter temperature playing a only minor role. Despite this, it should be noted that it is typically the motor temperature limit that is exceeded during flights, as opposed to the battery.

Figure 18 represents the impact of battery SOH on final SOC. The SOH was varied from 70% to 100% (the lowest value in flight tests was 67%). The final SOC ranges from 52% to 64% approx., a total fluctuation of 12%, indicating a significant impact of SOH on final SOC as expected.

### B. KPOC to KWJF

To fully demonstrate the simulation of key metrics required for energy-management by the developed framework, a case-study is presented to illustrate how these related to real-world mission requirements. This flight is performed between Brackett Field Airport (KPOC) (34.09132, -117.78218) and General Wm. J. Fox Airfield (KWJF) (34.73902, -118.21814). This route is of particular interest due to the mountain range located between these airports. Two different flight routes are considered from KPOC to KWJF; (1) a shortest route over the mountain range resulting a higher cruise altitude and (2) a flight through the West of the mountain range which results in a lower required altitude but a further flight distance. These trajectories can be seen in Figure 22 where the pentagon shows the location of KPOC and the cross the destination airport KWJF. Again, units of the figure are in pixels to facilitate image extraction from the terrain file and nearby airports 'A' and heliports 'H' are identified. Figure 23 shows the 3D trajectories of the two routes.

In comparison to the canonical A-B mission that will typically exemplify electric GA flights presented previously,



**Fig. 14 Flight Route from KVNY to KTOA**

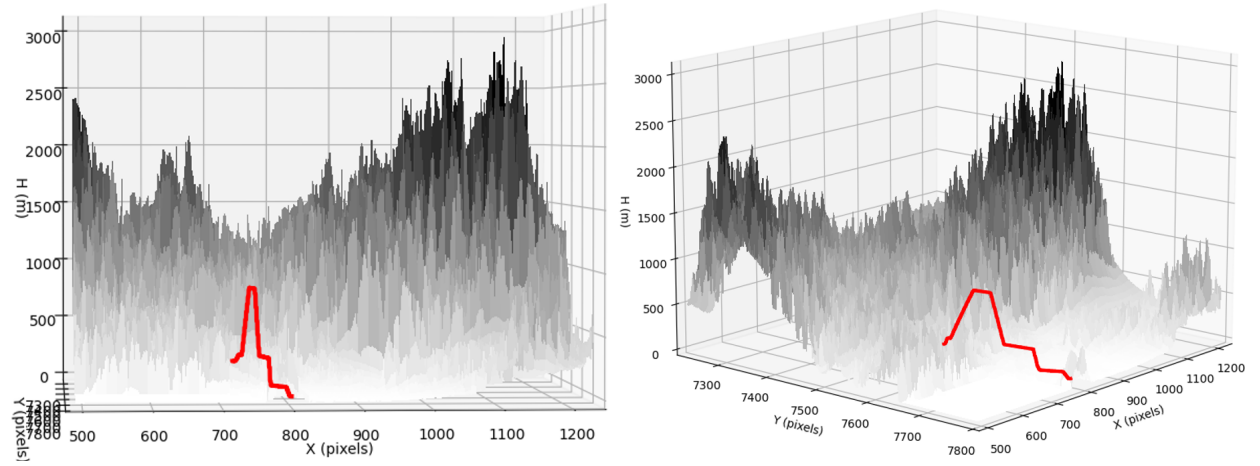


**Fig. 15 3D Flight Profile from KVNY to KTOA**

this case-study is designed to push the limits of the aircraft, including steep climb segments over challenging terrain. The selection of two alternate routes to complete the mission helps to assess the impact of parameters discussed - such as OAT, SOH, and initial component temperatures - as only some routes will prove suitable for certain conditions, as is the case for real operations.

Both routes are first flown at optimal conditions - ISA standard day of 15°C, an initial SOC and SOH of 100% , with initial battery temperature at ambient, and initial inverter and motor temperatures ambient +5°C and ambient +10°C respectively. Figure 24 depicts the simulated trajectories for scenario (1), where the vehicle attempts to take the



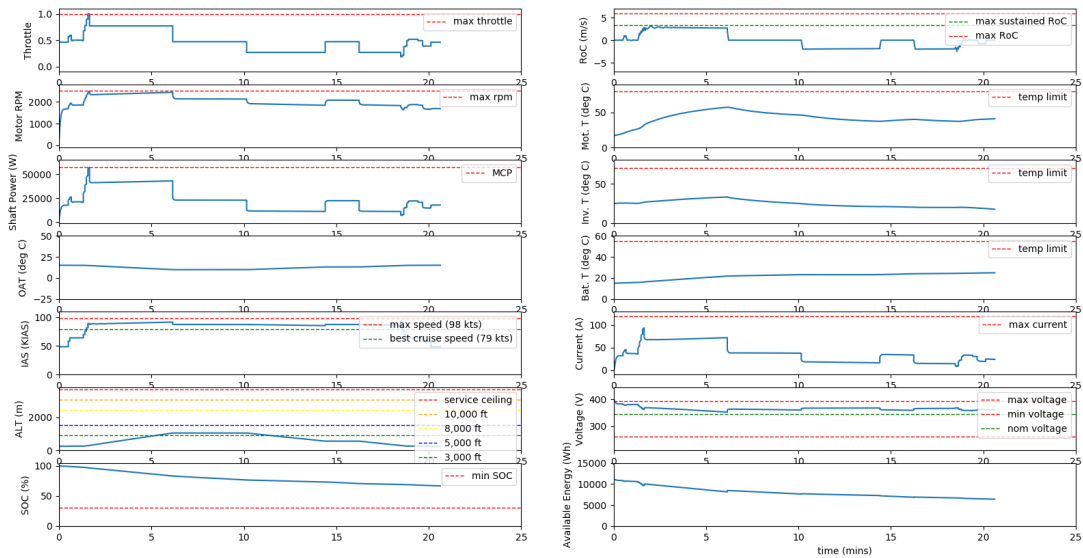


**Fig. 16 Simulated Powertrain Metrics for A-to-B Mission from Van Nuys Airport to Zamperini Field**

A to B Van Nuys Airport (VNY) to Zamperini Field (TOA) for range of OAT

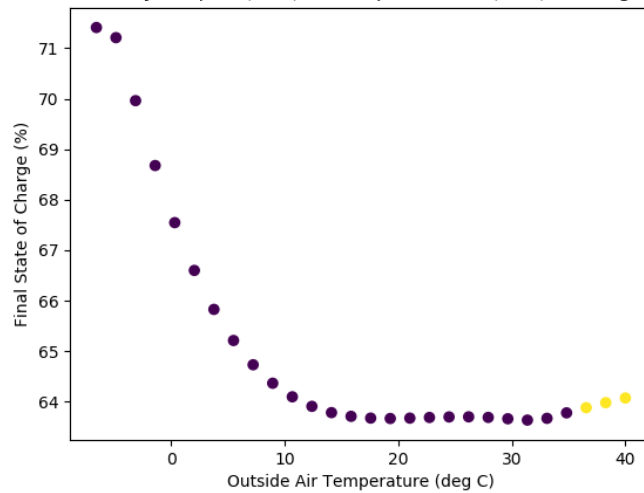


**Fig. 17 Final State of Charge for A-to-B Mission across range of OAT (Yellow Denotes Runs Where Motor Temperature Limit is Exceeded)**

shortest direct route, by sustaining a high cruise altitude to clear the mountains. The simulated power metrics are shown in Figure 25, where it can be observed that although the mission successfully completes at just above the minimum recommended final SOC of 30% (final SOC of 35%), the aggressive climb over the mountain nearly exceeds the motor temperature limit for a standard day.

In comparison, scenario (2) attempts to fly around the most difficult terrain, reducing the thermal burden on the powertrain but increasing total flight distance. This simulated trajectory is shown in Figure 26, and the effects on the resultant powertrain metrics can be observed in Figure 27. For this scenario, it is observed that a much longer flight time is required, and the final SOC is lower than scenario (1), at 20%, vs 35%. Despite this decrease in performance,

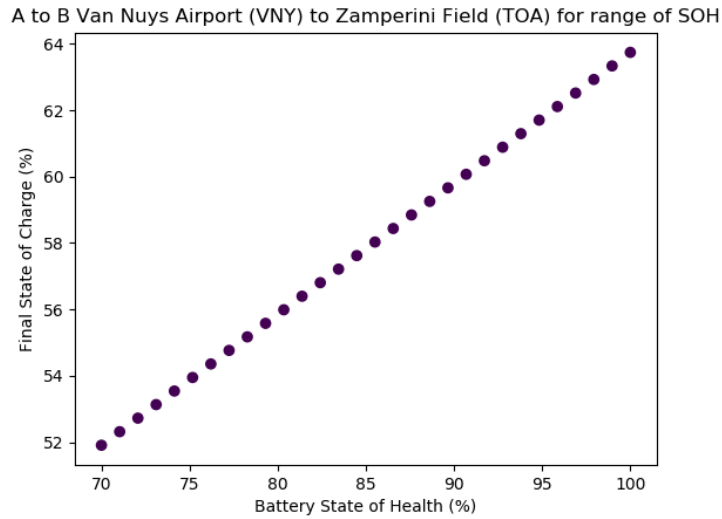


**Fig. 18 Final State of Charge for A-to-B Mission across range of SOH**

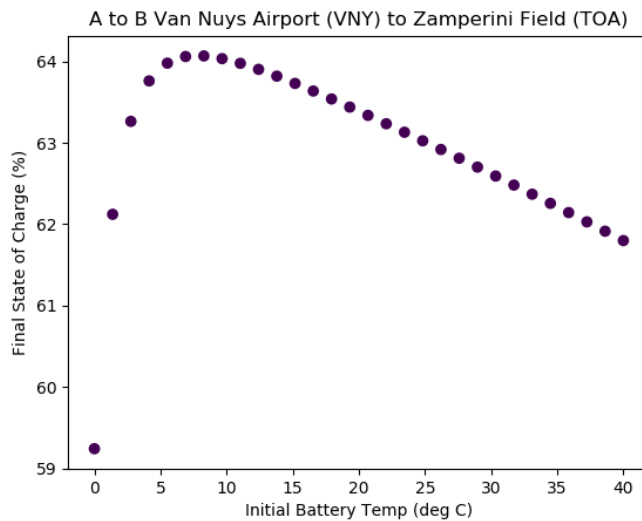


**Fig. 19 Final State of Charge for A-to-B Mission Across Range of Initial Battery Temperatures**

it should be also noted that the temperature limits are not in danger of being exceeded, indicating that although this scenario will strain the battery by dipping below the recommended minimum, the instantaneous performance of the powertrain is likely to be preferable, given the lower component temperatures.

This can be further compared by rerunning these scenarios at a higher ambient temperature. Instead, utilizing atmospheric conditions of ISA, scenario (1) was flown again at ISA -25°C, and ISA +25 °C. The simulated powertrain metrics for each are shown in Figures 28 and 29 respectively. It can be observed that this scenario suffers heavily on a hot day, with the motor temperature limit being exceeded for nearly 10 minutes - something that would clearly not be feasible. On the other hand, flying this scenario on a particularly cold day did not significantly impact the overall performance.

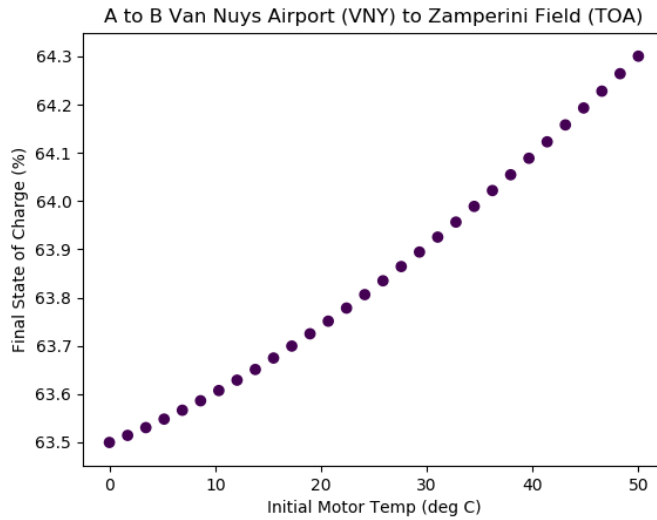


**Fig. 20 Final State of Charge for A-to-B Mission Across Range of Initial Motor Temperatures**

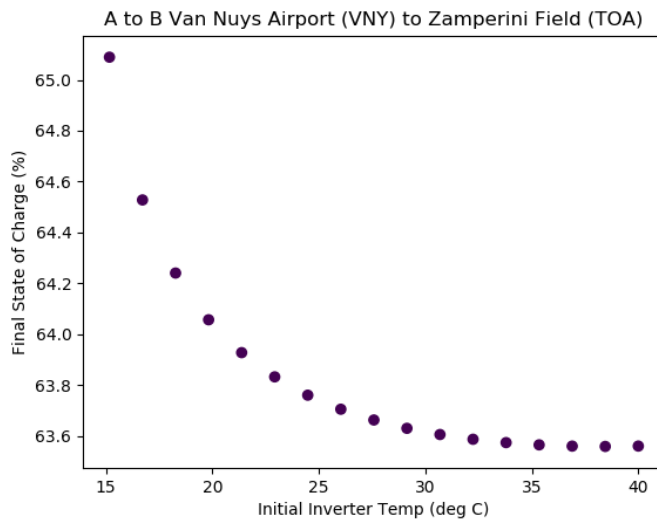


**Fig. 21 Final State of Charge for A-to-B Mission Across Range of Initial Inverter Temperatures**

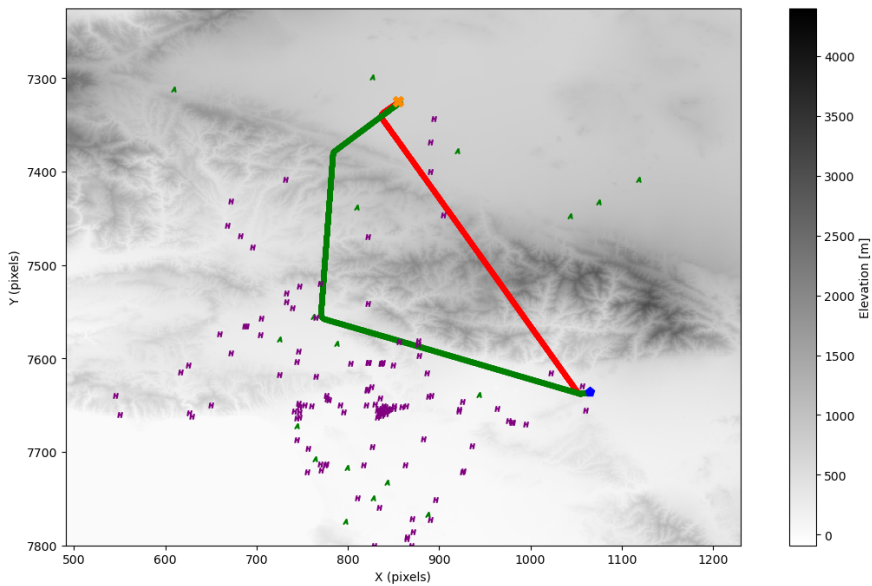


**Fig. 22 Flight Routes from KPOC to KWJF**

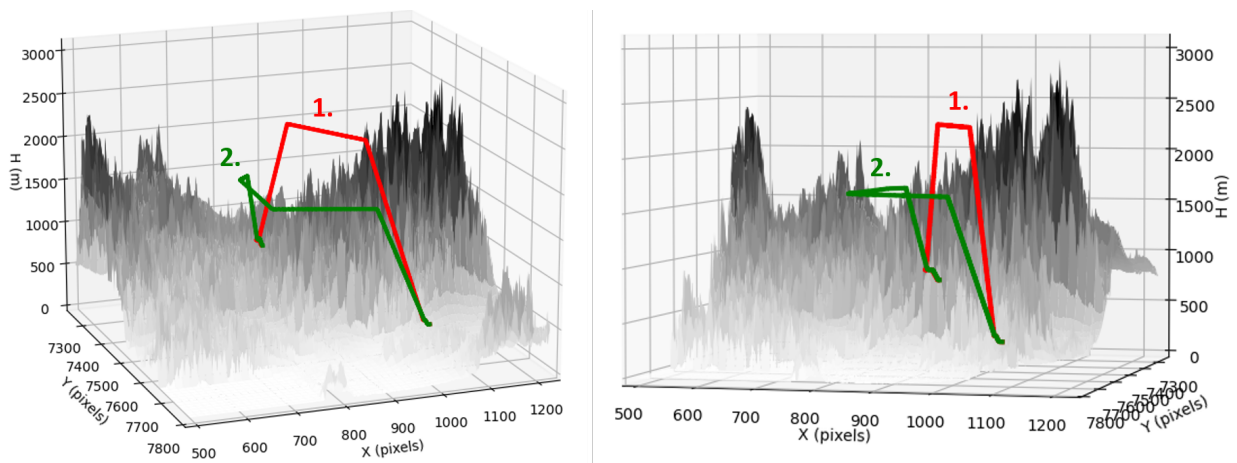


**Fig. 23 3D Flight Profiles from KPOC to KWJF**

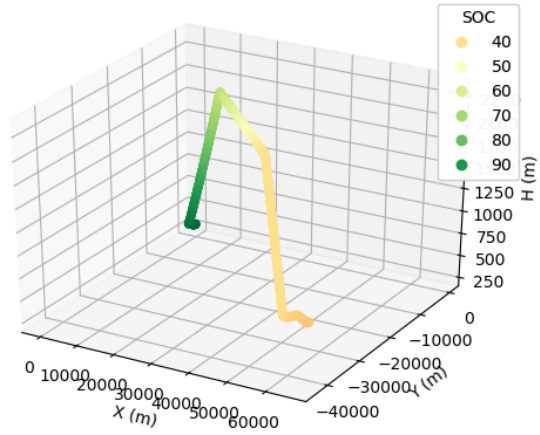


**Fig. 24 Simulated Trajectory for KPOC to KWJF (1) at ISA**

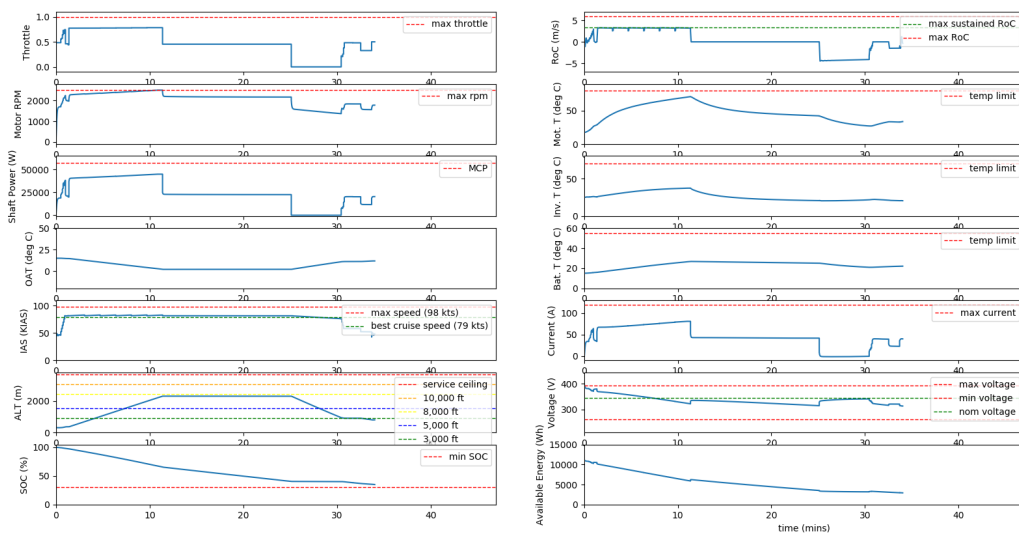


**Fig. 25 Simulated Powertrain Metrics for KPOC to KWJF (1) at ISA**

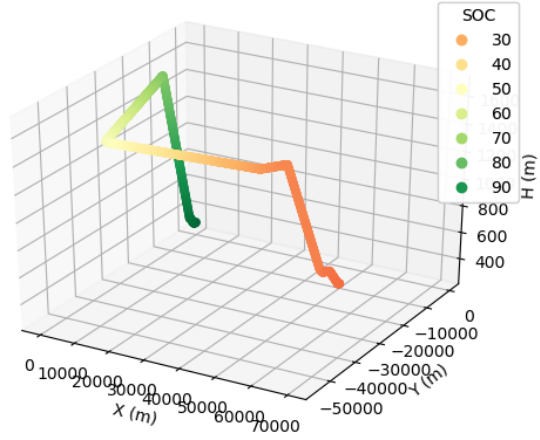


Fig. 26 Simulated Trajectory for KPOC to KWJF (2) at ISA

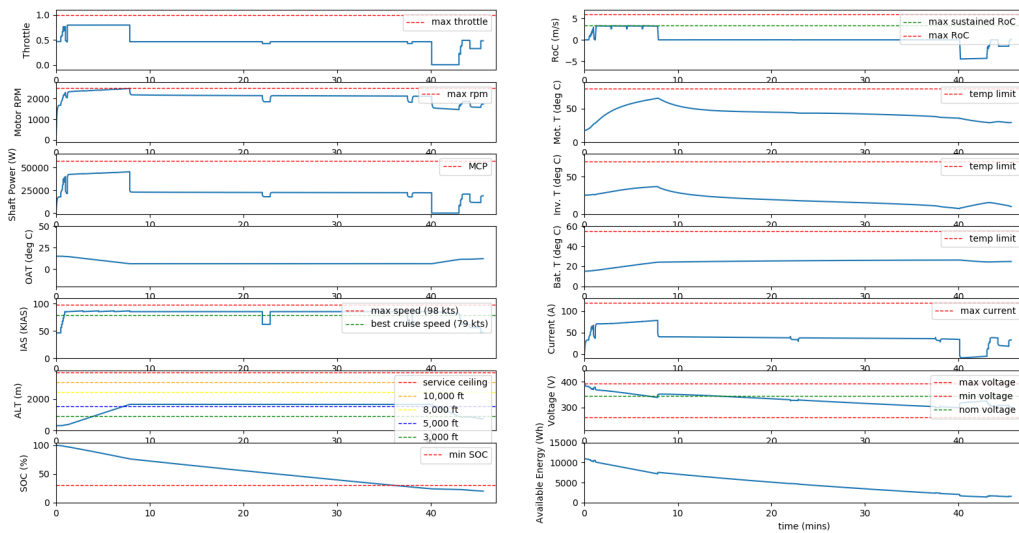
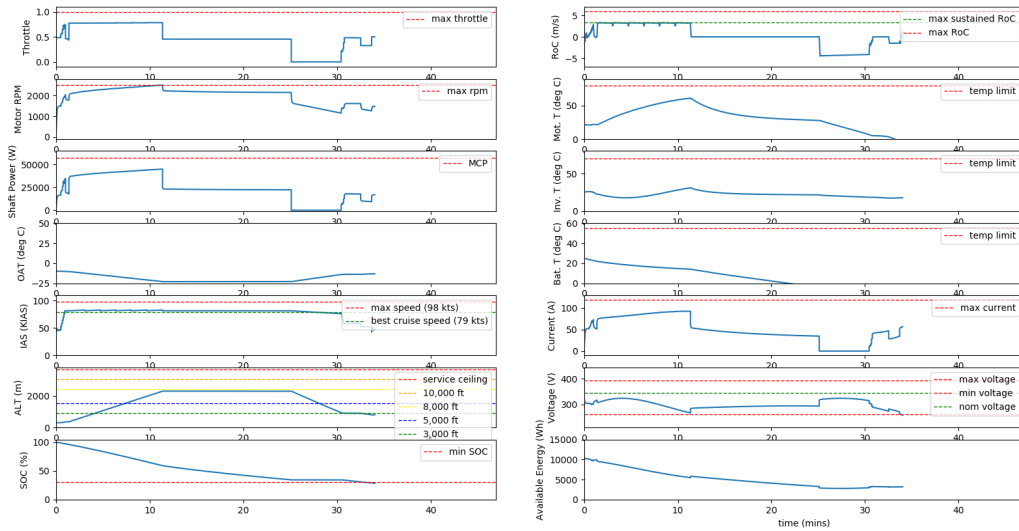
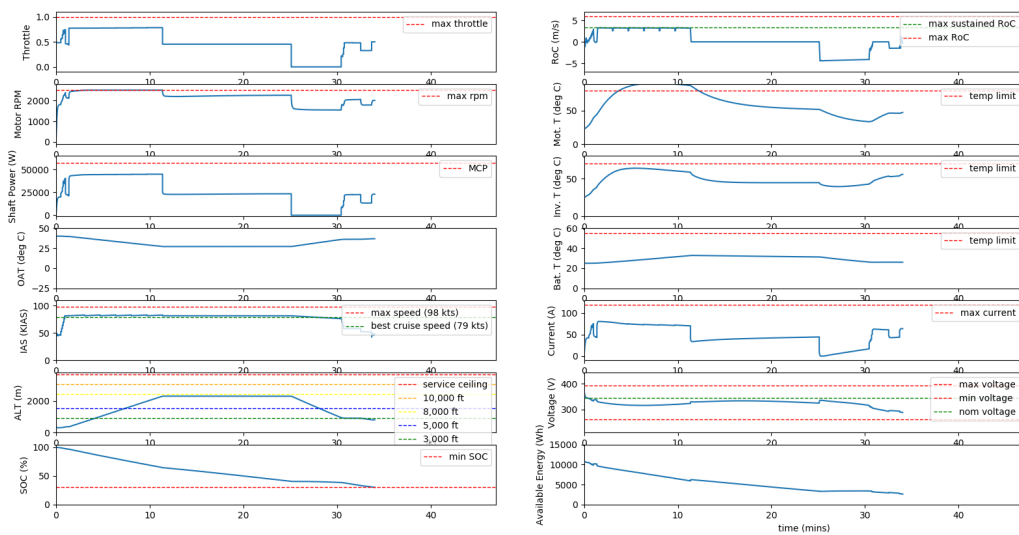


Fig. 27 Simulated Powertrain Metrics for KPOC to KWJF (2) at ISA



**Fig. 28 Simulated Powertrain Metrics for KPOC to KWJF (1) at ISA -25°C**



**Fig. 29 Simulated Powertrain Metrics for KPOC to KWJF (1) at ISA +25°C**

## VI. Conclusion

A framework has been developed combining the capabilities of a flight-dynamics model and electric powertrain model. This integrated framework was validated against real-world flight test data for a notional two-seater electric aircraft, closely matching the trajectory and key energy metrics such as SOC. Each of these capabilities was demonstrated. Firstly, the flight-dynamics model proved capable of not only simulating notional flights, but recreating trajectories flown by contemporary electric aircraft and matching key parameters. Secondly, The powertrain model accurately simulated key metrics (such as SOC, energy, current, and voltage) for the notional two-seat electric aircraft used to train the surrogate models.

The capability of the integrated environment has been demonstrated with a canonical A-B mission profile, and the impact of key parameters assessed with repeated flights. Outside air temperature, initial battery temperature, and State of Health were all identified as key metrics impacting the final state of charge. This mission represented the kind of short range A-B flight typical of an electric GA, and depicted a commuter flight from Van Nuys to Zamperini Field in Los Angeles. Further case-studies depicting two alternate routes were used to further quantify performance of the modeled aircraft - these represented a mountain crossing using a direct and indirect approach. It was shown that the model was capable of crossing the mountains directly, and landing at approximately 30% final SOC - the recommended minimum. However, it was shown that flying this same mission on a hot day or with an unhealthy battery can result in an infeasible mission. These are the kind of trade offs that demonstrate the utility of the existing environment, and further motivate the development of the work presented here into a full TEM environment.

Future work will include VTOL aircraft and lift-to-cruise transitioning aircraft in the evaluation environment. Additionally, two techniques of trajectory formation will be investigated. First, energy-optimal flight paths from point A to point B, or a subset of points such as regional airports. Second, exploration of flight paths in the local map limited by terrain, energy, and thermal constraints. This capability could provide accurate estimates on where the vehicle can navigate to at any point in time, which may be critical for fully-electric aircraft pilots or flight planners. The Rapidly Exploring Random Tree (RRT) algorithm will be modified to include energy metrics and kinodynamic constraints to provide insight on accessible flight paths, such as with Alternative Routing RRT\* [22].



## Acknowledgments

The authors would like to acknowledge the feedback received throughout this research from Ross Schaller. The authors also express their profound gratitude to Alberto Favier and Tine Tomazic from Pipistrel Aircraft, for kindly providing flight test data, and a wealth of knowledge that helped to make this research possible.

## References

- [1] Puranik, T., Jimenez, H., and Mavris, D., “Energy-based metrics for safety analysis of general aviation operations,” *Journal of Aircraft*, Vol. 54, No. 6, 2017, pp. 2285–2297.
- [2] Brelje, B. J., and Martins, J. R., “Electric, hybrid, and turboelectric fixed-wing aircraft: A review of concepts, models, and design approaches,” *Progress in Aerospace Sciences*, Vol. 104, 2019, pp. 1–19.
- [3] Patterson, M. D., German, B. J., and Moore, M. D., “Performance analysis and design of on-demand electric aircraft concepts,” *12th AIAA Aviation Technology, Integration, and Operations (ATIO) Conference and 14th AIAA/ISSMO Multidisciplinary Analysis and Optimization Conference*, 2012.
- [4] Chin, J. C., Schnulo, S. L., Miller, T. B., Prokopius, K., and Gray, J., “Battery Performance Modeling on Maxwell X-57,” *AIAA Scitech 2019 Forum*, AIAA Aviation, American Institute of Aeronautics and Astronautics, 2019.
- [5] Singh, R., Perullo, C., and Mavris, D., “A review of hybrid-electric energy management and its inclusion in vehicle sizing,” *Aircraft Engineering and Aerospace Technology: An International Journal*, 2014.
- [6] Falck, R. D., Chin, J., Schnulo, S. L., Burt, J. M., and Gray, J. S., “Trajectory optimization of electric aircraft subject to subsystem thermal constraints,” *18th AIAA/ISSMO Multidisciplinary Analysis and Optimization Conference*, 2017, p. 4002.
- [7] Schnulo, S. L., Chin, J. C., Falck, R. D., Gray, J. S., Papathakis, K. V., Clarke, S., Reid, N., and Borer, N. K., “Development of a Multi-Phase Mission Planning Tool for NASA X-57 Maxwell,” *Electric Aircraft Technology Symposium*, AIAA, 2018, pp. 1–14.
- [8] Fotouhi, A., Auger, D. J., Propp, K., Longo, S., and Wild, M., “A review on electric vehicle battery modelling: From Lithium-ion toward Lithium–Sulphur,” *Renewable and Sustainable Energy Reviews*, Vol. 56, 2016, pp. 1008–1021.
- [9] Rivera-Barrera, J. P., Muñoz-Galeano, N., and Sarmiento-Maldonado, H. O., “SoC estimation for lithium-ion batteries: Review and future challenges,” *Electronics*, Vol. 6, No. 4, 2017, p. 102.
- [10] Shrivastava, P., Soon, T. K., Idris, M. Y. I. B., and Mekhilef, S., “Overview of model-based online state-of-charge estimation using Kalman filter family for lithium-ion batteries,” *Renewable and Sustainable Energy Reviews*, Vol. 113, 2019, p. 109233.
- [11] Aircraft, P., “Velis Electro EASA TC,” , 2020. URL <https://www.pipistrel-aircraft.com/aircraft/electric-flight/velis-electro-easa-tc/>, commercial website.
- [12] Agency, E. U. A. S., “Type-Certificate Data Sheet No. EASA.A.573,” , 2020. URL [https://www.easa.europa.eu/sites/default/files/dfu/tcds\\_easa.a.573\\_is.5\\_0.pdf](https://www.easa.europa.eu/sites/default/files/dfu/tcds_easa.a.573_is.5_0.pdf), type-Certificate Data Sheet.
- [13] Aircraft, P., “Pipistrel-Velis-Electro3,” , 2020. URL <https://www.pipistrel-aircraft.com/aircraft/electric-flight/velis-electro-easa-tc/#prev>, image.
- [14] How, D. N., Hannan, M., Lipu, M. H., and Ker, P. J., “State of charge estimation for lithium-ion batteries using model-based and data-driven methods: A review,” *IEEE Access*, Vol. 7, 2019, pp. 136116–136136.
- [15] Stengel, R. F., *Flight Dynamics*, 1<sup>st</sup> ed., Princeton University Press, New York, 2005, Chaps. 1,2,3,4.
- [16] Marco, A. D., Duke, E., and Berndt, J., “A General Solution to the Aircraft Trim Problem,” *AIAA Modeling and Simulation Technologies Conference and Exhibit*, 2012. <https://doi.org/10.2514/6.2007-6703>, URL <https://arc.aiaa.org/doi/abs/10.2514/6.2007-6703>.
- [17] Klesh, A., and Kabamba, P., “Solar-Powered Aircraft: Energy-Optimal Path Planning and Perpetual Endurance,” *Journal of Guidance Control and Dynamics*, Vol. 32, 2009, pp. 1320–1329.
- [18] Al-Sabban, W. H., Gonzalez, L. F., and Smith, R. N., “Wind-energy based path planning for Unmanned Aerial Vehicles using Markov Decision Processes,” *2013 IEEE International Conference on Robotics and Automation*, 2013, pp. 784–789. <https://doi.org/10.1109/ICRA.2013.6630662>.

- [19] Pettersson, P., and Doherty, P., “Probabilistic Roadmap Based Path Planning for an Autonomous Unmanned Helicopter,” *Journal of Intelligent and Fuzzy Systems*, Vol. 17, No. 4, 2006, pp. 395–4052.
- [20] LaValle, S. M., and Kuffner Jr, J. J., “Randomized kinodynamic planning,” *The international journal of robotics research*, Vol. 20, No. 5, 2001, pp. 378–400.
- [21] Lin, Y., and Saripalli, S., “Sampling-Based Path Planning for UAV Collision Avoidance,” *IEEE Transactions on Intelligent Transportation Systems*, Vol. 18, No. 11, 2017, pp. 3179–3192. <https://doi.org/10.1109/TITS.2017.2673778>.
- [22] Choudhury, S., Scherer, S., and Singh, S., “Realtime Alternate Routes Planning: The RRT\*-AR Algorithm,” 2012.
- [23] Pereira, G. A. S., Choudhury, S., and Scherer, S., “Kinodynamic Motion Planning on Vector Fields using RRT\*,” Tech. Rep. CMU-RI-TR-16-35, Carnegie Mellon University, Pittsburgh, PA, July 2016.
- [24] GAMA, “GAMA PUBLICATION NO. 16; HYBRID AND ELECTRIC PROPULSION PERFORMANCE MEASUREMENT,” Tech. rep., General Aviation Manufacturers Association, Washington, DC USA, February 2017. URL <https://gama.aero/wp-content/uploads/GAMA-Publication-No-16-Hybrid-and-Electric-Propulsion-Performance-Measurement-1.pdf>.